SPANDIDOS PUBLICATIONS

ONCOLOGY REPORTS 49: 64, 2023

HOXA-AS3 induces tumor progression through the epithelial-mesenchymal transition pathway in epithelial ovarian cancer

KYUNG JIN EOH[1], DAE WOO LEE[2], EUN JI NAM[3], JAE IN KIM[3], HANNA MOON[3], SANG WUN KIM[3] and YOUNG TAE KIM[3]

[1]Department of Obstetrics and Gynecology, Center for Digital Health, Yongin Severance Hospital, Yonsei University College of Medicine, Yongin, Gyeonggi-do 16995; [2]Department of Obstetrics and Gynecology, Bucheon St. Mary's Hospital, College of Medicine, Catholic University of Korea, Bucheon, Gyeonggi-do 14647; [3]Department of Obstetrics and Gynecology, Institute of Women's Medical Life Science, Yonsei Cancer Center, Severance Hospital, Yonsei University College of Medicine, Seoul 03722, Republic of Korea

Received May 3, 2022; Accepted November 18, 2022

DOI: 10.3892/or.2023.8501

Abstract. HOXA cluster antisense RNA 3 (HOXA-AS3) is considered to be involved in several malignancies, however, its biological function in the progression of epithelial ovarian cancer (EOC) remains unclear. The present study compared the expression of HOXA-AS3 in ovarian cancer and normal ovarian tissues and analyzed the association between the expression of HOXA-AS3 and the survival outcomes of patients with ovarian cancer. RNA interference was used to suppress HOXA-AS3 expression in ovarian cancer cell lines in order to demonstrate the function of HOXA-AS3 in ovarian cancer progression. The associations between HOXA-AS3 and epithelial-mesenchymal transition (EMT) markers were explored to verify the mechanism of action of HOXA-AS3 in ovarian cancer. The results of the present study revealed that ovarian cancer tissues exhibited higher HOXA-AS3 expression than normal ovarian tissues. Clinical data indicated that HOXA-AS3 was a significant predictor of progression-free survival and overall survival. Patients with high HOXA-AS3 expression had a poorer prognosis than patients with low HOXA-AS3 expression. *In vitro* experiments using HOXA-AS3-knockdown ovarian cancer cell lines demonstrated that HOXA-AS3 knockdown inhibited cell proliferation and migration. HOXA-AS3 was a potent inducer and modulator of the expression of EMT pathway-related markers and interacted with both the mRNA and protein forms of HOXA3. Collectively, the findings of the present study demonstrated that HOXA-AS3 expression is associated with ovarian cancer progression and thus, may be employed as a prognostic marker and therapeutic target in EOC.

Correspondence to: Dr Young Tae Kim, Department of Obstetrics and Gynecology, Institute of Women's Medical Life Science, Yonsei Cancer Center, Severance Hospital, Yonsei University College of Medicine, 50-1 Yonsei-Ro, Seoul 03722, Republic of Korea
E-mail: ytkchoi@yuhs.ac

Abbreviations: HOXA-AS3, HOXA cluster antisense RNA 3; EMT, epithelial-mesenchymal transition; lncRNAs, long noncoding RNAs; siRNA, small interfering RNA; siNC, negative control siRNA; RT-qPCR, reverse transcription-quantitative polymerase chain reaction; CCK-8, Cell Counting Kit-8; PBS, phosphate-buffered saline

Key words: HOXA-AS3, long noncoding RNA, progression, prognosis, ovarian cancer

Introduction

Ovarian cancer is generally diagnosed at an advanced stage, and is thus the leading cause of mortality in women diagnosed with gynecologic cancer (1). Despite the progress in systemic therapies in the past few years, the long-term prognosis of patients with ovarian cancer remains poor. Understanding the molecular mechanisms that are involved in ovarian cancer progression may lead to the development of more effective cancer treatments.

Aberrant lncRNA expression has been identified in numerous types of diseases, including cancer (2). Long noncoding RNAs (lncRNAs) are transcripts of >200 nucleotides without protein-coding functions (2). LncRNAs play a role in regulating cancer cell proliferation, differentiation, invasion, and metastasis (3,4). Additionally, epithelial-mesenchymal transition (EMT) has been increasingly investigated in various types of cancer. Epithelial cells lose apical-basal polarity, cell-cell adhesion, and acquire migration properties to transform into invasive mesenchymal cells during EMT (5,6). However, it remains unclear whether EMT is involved in the lncRNA-mediated progression of epithelial ovarian cancer (EOC).

HOXA cluster antisense RNA 3 (HOXA-AS3) belongs to the family of homeobox (HOX) genes characterized by the presence of highly conserved homeodomains, which are essential for embryonic development and tumorigenesis. Several studies have investigated the role of HOXA-AS3 in the

carcinogenesis of gliomas and lung cancers (7-9). Although HOXA-AS3 has been demonstrated to be associated with the progression of other types of cancer, little is known about its involvement in the molecular pathways of ovarian cancer cells.

In the present study, the role and underlying mechanisms of lncRNAs in ovarian cancer were investigated with a focus on HOXA-AS3, which is highly expressed in ovarian cancer.

Materials and methods

Patient specimens. Ovarian cancer tissue and matched benign tissue specimens were collected from 130 patients who underwent surgery at the Department of Obstetrics and Gynecology, Severance Hospital (Seoul, Korea), between January 2005 and December 2017. The inclusion criteria was as follows: i) Aged ≥19 years; ii) pathologically confirmed EOC; and iii) underwent primary treatment, either primary debulking surgery followed by platinum-based postoperative adjuvant chemotherapy or platinum-based neoadjuvant chemotherapy followed by interval debulking surgery and postoperative adjuvant chemotherapy. In addition, patients were excluded from the present study, according to the following criteria: i) Were immunocompromised or pregnant; ii) did not receive platinum-based combination chemotherapy; iii) had synchronous double primary cancers; and iv) were lost to follow-up before reaching six months of progression-free survival (PFS) without evidence of disease recurrence. The clinicopathological characteristics of the patients (age range, 32-78 years; mean age, 51±12.4 years) are presented in Table I. All tissue samples were immediately frozen in liquid nitrogen and transferred to a -80˚C deep freezer. Patient follow-up information and survival were determined based on the medical records. The study was approved (approval ethics code 4-2021-1394) by the Institutional Review Board of Severance Hospital, Yonsei University College of Medicine. Individual patient consent was waived for the present study because it was a retrospective study which involved no risk to the subjects.

Cell culture. Human Ovarian Surface Epithelial Cells (cat. no. 7310; Sciencell Research Laboratories, Inc.) were cultured using OepiCM, which consisted of basal medium, 5 ml of Ovarian Epithelial Cell Growth Supplement (OEpiCGS; cat. no. 7352) and 1% penicillin/streptomycin solution (cat. no. 0503), and incubated at 37˚C in a humidified atmosphere containing 5% CO_2. Human EOC cell line A2780 (cat. no. 93112519) was purchased from the European Collection of Cell Cultures (ECACC; Sigma-Aldrich; Merck KGaA) and cultured in RPMI-1640 medium supplemented with 10% fetal bovine serum (FBS) and 1% penicillin/streptomycin (pen/strep; all from Gibco; Thermo Fisher Scientific, Inc.). OVCA429 and OVCA433 were provided by the Korea Gynecologic Cancer Bank through the Bio and Medical Technology Development Program of the Ministry of Science of Korea, Information and Communication Technology and Future Planning (10,11). These cell lines were cultured in Dulbecco's modified Eagle's medium (DMEM; Welgene, Inc.) containing 10% FBS and 1% pen/strep in an incubator at 37˚C with 5% CO_2.

Small interfering RNA (siRNA) transfection. siRNAs targeting HOXA-AS3 (si-HOXA-AS3-651 sense, 5'-UCUAUUCUCCAAGGGAAATT-3' and antisense, 5'-UUUCCCUUGCGAGAAUAGATT-3'; si-HOXA-AS3-728 sense, 5'-GGGCCGAACAACUCAUAAATT-3'and antisense, 5'-UUUAUGAGUUGUUCGGCCCTT-3'; si-HOXA-AS3-3507 sense, 5'-GCACAGAAUCUCAACUUUATT-3' and antisense, 5'-UAAAGUUGAGAUUCUGUGCTT-3'; all from Bioneer Corporation), HOXA3 (sense, 5'-GGUAGAUUCAUAGAAUAUAAC-3' and antisense, 5'-GUUAUAUUCUAUGAAUCUACC-3'; cat. no. sc-38675; Santa Cruz Biotechnology, Inc.) and negative control siRNA (siNC; cat. no. SN-1011; Bioneer Corporation) were used. The target sequence for HOXA-AS3 was as follows: 5'-GGUAGAUUCAUAGAAUAUAAC-3'. Both OVCA429 and OVCA433 cells were cultured to 80% confluency, and the transfection was performed at a concentration of 30 nM of siRNAs in 6-well plates at $1x10^5$ cells/well using Lipofectamine™ 3000 Transfection Reagent (Invitrogen; Thermo Fisher Scientific, Inc.) in Opti-MEM I Reduced Serum Medium (Gibco; Thermo Fisher Scientific, Inc.) according to the manufacturer's instructions at 37˚C for 48 h. The time interval between transfection and subsequent experimentation was 48 h.

RNA extraction and reverse transcription-quantitative polymerase chain reaction (RT-qPCR). Total RNA was extracted from cancerous and non-cancerous specimens and cell lines using TRIzol® reagent (cat. no. 15596026; Invitrogen; Thermo Fisher Scientific, Inc.). RNA concentration and quality were determined using a NanoDrop ND-2000 spectrophotometer (cat. no. ND-2000; NanoDrop Technologies; Thermo Fisher Scientific, Inc.). Total RNA (1 μg) was reverse transcribed into first-strand cDNA using a reverse transcription reagent kit (TaqMan™ Reverse Transcription Reagents; cat. no. N8080234; Invitrogen; Thermo Fisher Scientific, Inc.) according to the manufacturer's protocol. RT-qPCR was carried out in 96-well blocks with the StepOnePlus™ Real-Time PCR System (cat. no. 4376600; Applied Biosystems; Thermo Fisher Scientific, Inc.) using SensiFAST™ SYBR® Hi-ROX (cat. no. BIO-73001; Meridian Bioscience, Inc.) in a reaction volume of 20 μl. The following PCR program was used: An initial denaturation at 95˚C for 2 min, followed by 40 cycles of 5 sec at 95˚C and 60˚C for 15 sec. 18S rRNA and GAPDH were used as internal controls. The PCR primer sequences were as follows: 18S rRNA sense, 5'-GTAACCCGTTGAACCCCATT-3' and antisense, 5'-CCATCCAATCGGTAGTAGCG-3'; GAPDH sense, 5'-ACCCACTCCTCCACCTTTGA-3' and antisense, 5'-CTGTTGCTGTAGCCAAATTCGT-3'; HOXA-AS3 sense, 5'-TTCATCCGCTGCATCCAAGG-3' and antisense, 5'-AGAGAGGTGTCTGAAGCGCT-3'; HOXA3 sense, 5'-CAGCTCATGAAACGGTCTGC-3' and antisense, 5'-GAGCTGTCGTAGTAGGTCGC-3'; HOXA4 sense, 5'-ATAACGGAGGGGAGCCTAAG-3' and antisense, 5'-GCTCAGACAAACAGAGCGTG-3'; HOXA5 sense, 5'-CCAGATCTACCCCTGGATGC-3' and antisense, 5'-ACTTCATTCTCCGGTTTTGGAAC-3'; HOXA6 sense, 5'-AAGCACTCCATGACGAAGGC-3' and antisense, 5'-GTCTGGTAGCGCGTGTAGGT-3'. Changes in the expression levels were analyzed using the $2^{-\Delta\Delta Cq}$ method (12).

Cell viability assay. HOXA-AS3 siRNA-transfected cells were seeded into 96-well flat-bottomed plates at a density of $5x10^3$ cells per well in 200 μl of culture medium. Cell

Table I. HOXA-AS3 expression and clinicopathological characteristics of patients with ovarian cancer.

Parameters	Total (n=100)	HOXA-AS3 expression		P-value
		Low (n=50)	High (n=50)	
Age (years), mean ± SD	51.3±12.4	52.1±10.1	50.4±11.7	0.617
Stage, n (%)				
I	21 (21.0)	16 (32.0)	5 (10.0)	0.05
II	16 (16.0)	11 (22.0)	5 (10.0)	
III	48 (48.0)	18 (36.0)	30 (60.0)	
IV	15 (15.0)	5 (10.0)	10 (20.0)	
Grade, n (%)				
1	13 (13.0)	9 (18.0)	4 (8.0)	0.323
2	35 (35.0)	17 (34.0)	18 (36.0)	
3	52 (52.0)	24 (48.0)	28 (56.0)	
Histological type, n (%)				
Serous	64 (64.0)	31 (62.0)	33 (66.0)	0.710
Endometrioid	15 (15.0)	6 (12.0)	9 (18.0)	
Clear cell	14 (14.0)	9 (18.0)	5 (10.0)	
Mucinous	4 (4.0)	2 (4.0)	2 (4.0)	
Others	3 (3.0)	2 (4.0)	1 (2.0)	
Lymph node metastasis, n (%)	42 (42.0)	15 (30.0)	27 (54.0)	0.015
Recurrence, n (%)	58 (58.0)	23 (46.0)	35 (70.0)	0.015
CA 125 ≥200, n (%)	68 (68.0)	31 (62.0)	37 (74.0)	0.198

HOXA-AS3, HOXA cluster antisense RNA 3; CA 125, cancer antigen 125.

proliferation was evaluated using the Cell Counting Kit-8 (CCK-8) assay (Dojindo Molecular Technologies, Inc.) in accordance with the manufacturer's instructions. The cells were incubated overnight to allow cell attachment and recovery. Subsequently, the cells were transfected with siHOXA-AS3 for 24, 48, or 72 h. A total of 20 μl of CCK-8 solution was added to each well of the plate and incubated for an additional 1 h. The absorbance was measured at 450 nm using a microplate reader. Three independent experiments were performed in triplicate.

Colony formation assay. To assess clonogenic ability, cells (OVCA429 and OVCA433) were incubated for 3 days in 12-well plates at a low density ($5x10^2$ cells per well) in a complete medium for 14 days. The medium was changed to culture medium every 3 days. The plates were washed with phosphate-buffered saline (PBS), fixed with ice-cold methanol for 20 min at room temperature, and stained with 0.1% crystal violet (Sigma-Aldrich; Merck KGaA) for 10 min at room temperature. The total number of colonies were counted manually using a light microscope (Olympus Corporation), and a colony was defined as 50 cells or more. Each experiment was performed on three independent occasions.

Wound healing assay. Cells (OVCA429 and OVCA433) were seeded into 6-well culture plates with serum-enriched medium and allowed to grow to 90% confluency. The serum-containing medium was removed, and the cells were serum-starved overnight. When the cells reached 100% confluence, artificial wounds were created by scratching the monolayer with a 200-μl pipette tip. After scratching, floating cells were washed with serum-free medium and replenished with fresh medium. Wound healing was investigated at 0, 24, and 48 h, and images were captured using a light microscope (Olympus Corporation) and quantified using ImageJ software (version 1.8.0_172; National Institutes of Health). Each experiment was repeated three times.

Western blotting. Total protein was isolated from ovarian cancer cell lines (OVCA429 and OVCA433) using radioimmunoprecipitation assay lysis and extraction buffer (Thermo Fisher Scientific, Inc.), and protein concentrations were quantified using the Pierce BCA Protein Assay Kit (Thermo Fisher Scientific, Inc.). Protein samples (20 μg) were separated on 12% sodium dodecyl sulfate-polyacrylamide gel electrophoresis gels and then transferred to polyvinylidene difluoride membranes (MilliporeSigma). The membranes were blocked with 5% skimmed milk in 1X Tris-buffered saline and 0.1% Tween®-20 (TBST) buffer for 1 h at room temperature and incubated with the primary antibody overnight at 4˚C with gentle rocking. The membrane was washed three times with 1X TBST buffer, followed by incubation with horseradish peroxidase-conjugated secondary antibodies (1:5,000; cat. nos. 7074 and 7076; Cell Signaling Technology, Inc.) for 2 h at room temperature. The primary antibodies used in this study were as follows: Anti-HOXA3 (1:1,000; cat. no. sc-374237; Santa Cruz Biotechnology, Inc.), anti-β-catenin (1:1,000; cat. no. 2698S), anti-E-cadherin (1:1,000; cat. no. 3195), anti-AKT (1:1,000; cat. no. 9272), anti-vimentin (1:1,000; cat. no. 5741; all Cell

Signaling Technology, Inc.), and β-actin antibody (1:5,000; cat. no. A5316; Sigma-Aldrich; Merck KGaA). The bands were visualized using an enhanced chemiluminescence solution (Pierce™ ECL Western Blotting Substrate; cat. no. 32106; Thermo Scientific™, Inc.) and analyzed using ImageJ software (version 1.8.0_172; National Institutes of Health).

Immunofluorescence analysis. OVCA429 and OVCA433 cells were cultured at a density of $5x10^3$ cells per confocal dish (SPL Life Sciences, Co., Ltd.). After incubation, the dishes were washed with PBS and fixed in 4% formaldehyde for 20 min at room temperature. The cells were then rinsed twice with PBS and blocked with blocking buffer (10% normal donkey serum; cat. no. 017-000-121; Jackson ImmunoResearch Laboratories, Inc.; and 0.3% Triton X-100) for 45 min at room temperature. The dishes were incubated with a primary antibody, overnight at 4°C, followed by incubation with the appropriate secondary fluorescence-labeled antibody for 1 h at room temperature. Nuclei were counterstained with DAPI (cat. no. D1306; Invitrogen; Thermo Fisher Scientidic, Inc.) for 5 min at room temperature. The images were visualized using a confocal microscope (Zeiss AG). The primary antibodies used in this study were as follows: Anti-HOXA3 (1:100; cat. no. ab230879; Abcam), anti-tubulin (1:100; cat. no. 2144; Cell Signaling Technology, Inc.). The secondary antibodies used in this study were as follows: Anti-rabbit Alexa Fluor 488 (1:100; cat. no. A-11008; Invitrogen; Thermo Fisher Scientific, Inc.) and Rhodamine Red anti-mouse (1:200; cat. no. 715-295-151; Jackson ImmunoResearch Laboratories, Inc.).

Statistical analysis. Statistical analyses were performed using SPSS version 25 for Windows (IBM Corp.). The Kolmogorov-Smirnov test was used to validate standard normal-distributional assumptions. Data are expressed as the mean ± standard deviation. Multiple comparsions among groups was performed using one-way ANOVA with Bonferroni correction and for comparisons between groups paired Student's t-test was used. Two-tailed P-values of <0.05 were considered to indicate a statistically significant difference. PFS and overall survival (OS) were calculated by Kaplan-Meier analysis using the log-rank test to determine significance. Statistical significance was set at P<0.05.

Results

Upregulation of HOXA-AS3 is associated with poor prognosis in EOC tissues and cells. To explore the function of HOXA-AS3 in ovarian cancer, HOXA-AS3 expression in ovarian cancer cell tissues and cells (A2780, OVCA429, and OVCA433) was detected by RT-qPCR. The results revealed that the expression of HOXA-AS3 was higher in ovarian cancer cells than in non-cancerous cells (Fig. 1A). Among them, HOXA-AS3 levels were higher in OVCA429 and OVCA433 cells and lowest in the A2780 cell line. For this reason, OVCA429 and OVCA433 cells were selected for further experiments. In addition, benign tissues and human ovarian surface epithelial cells were used as controls. The results revealed that lncRNA HOXA-AS3 expression was significantly higher in ovarian cancer tissue (n=100) than in the control (n=30) (Fig. 1B). The median relative expression levels of HOXA-AS3 were used to determine the cut-off values of the high and low HOXA-AS3 expression groups. Kaplan-Meier analysis indicated that patients with high HOXA-AS3 expression had worse OS and PFS compared to those with low HOXA-AS3 expression (Fig. 1C and D). The clinical characteristics of patients who were in the low (n=50) and high (n=50) HOXA-AS3 expression groups were also compared. Clinicopathological data, such as age, stage, grade, histological type, lymph node metastasis, recurrence, and cancer antigen (CA125) levels, were compared between the low and high expression groups (Table I). The results indicated that high expression of lncRNA HOXA-AS3 was associated with poor prognostic factors including lymph node metastasis and recurrence in patients with ovarian cancer.

Knockdown of HOXA-AS3 inhibits cell proliferation in ovarian cancer. To further investigate the biological function of HOXA-AS3 in ovarian cancer cell development and progression, the expression of HOXA-AS3 was knocked down in OVCA429 and OVCA433 cells by transfecting siRNA. The CCK-8 assay was performed to determine whether the knockdown of HOXA-AS3 suppressed cell proliferation in ovarian cancer cells. The results revealed that HOXA-AS3 knockdown significantly decreased the proliferation of OVCA429 and OVCA433 cells (Fig. 2A). In addition, the colony formation assay demonstrated that the cell proliferation rate decreased following HOXA-AS3 knockdown (Fig. 2B). Taken together, these results revealed that the knockdown of HOXA-AS3 significantly hindered ovarian cancer cell proliferation.

HOXA-AS3 promotes ovarian cancer cell migration. Wound healing assays were performed to investigate the effect of HOXA-AS3 on ovarian cancer cell migration. The results showed that HOXA-AS3 knockdown reduced the migration ability of OVCA429 and OVCA433 cells (Fig. 3A and B), indicating that HOXA-AS3 promoted cell migration in ovarian cancer. Silencing of HOXA-AS3 in OVCA429 and OVCA433 cell lines reduced scratch closure by 50 and 60%, respectively, compared with control cell lines at 48 h. Collectively, these results revealed that the knockdown of HOXA-AS3 significantly hindered cell migration.

HOXA-AS3 regulates the EMT signaling pathway in ovarian cancer cells. Numerous studies have revealed that the EMT signaling pathway plays a critical role in the modulation of cell proliferation and metastasis of cancers (5,6). To evaluate the role of HOXA-AS3 in EMT signaling, western blotting and RT-qPCR were performed (Fig. 4). The results of the western blot analysis demonstrated that HOXA-AS3 knockdown caused significant upregulation of E-cadherin and downregulation of β-catenin, AKT and vimetin in OVCA429 and OVCA433 cells compared with the cells in the siNC group (Fig. 4A and B). The mRNA levels of β-catenin, AKT, and vimentin were downregulated, and E-cadherin was upregulated following the knockdown of HOXA-AS3 in ovarian cancer (Fig. 4B). These results indicated that knockdown of HOXA-AS3 suppressed ovarian cancer cell proliferation and migration by inhibiting EMT signaling.

HOXA-AS3 regulates HOXA3 mRNA and protein. The knockdown of HOXA-AS3 upregulated HOXA3 expression

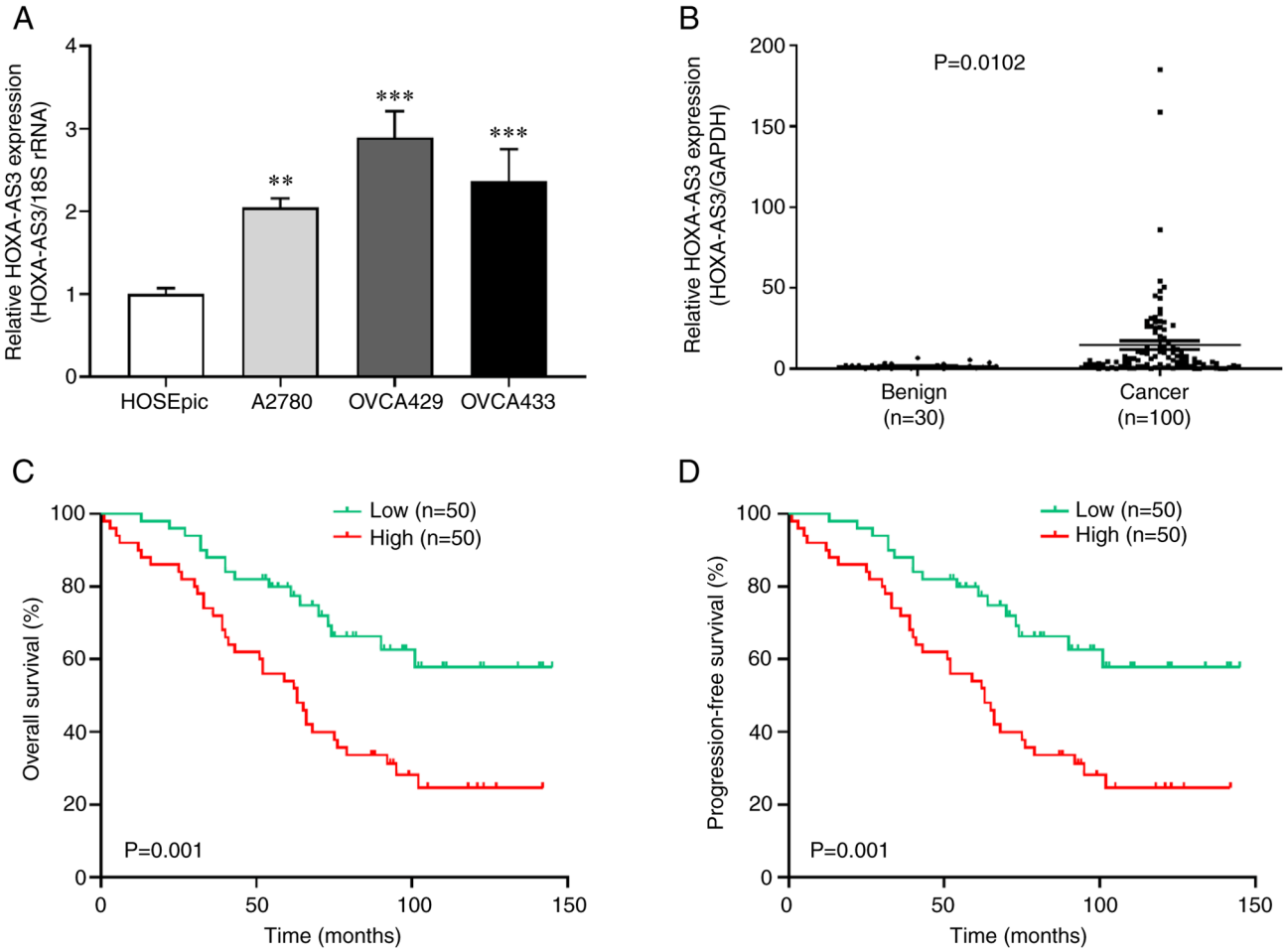

Figure 1. lncRNA HOXA-AS3 is upregulated in ovarian cancer tissues and associated with the poor prognosis of patients with ovarian cancer. (A) HOXA-AS3 expression level in ovarian cancer cell lines. (B) lncRNA HOXA-AS3 expression was assessed in ovarian cancer tissues (n=100) and adjacent normal tissues (n=30) using reverse transcription-quantitative polymerase chain reaction. (C and D) Kaplan-Meier survival analysis and log-rank testing were performed to analyze the (C) overall survical and (D) progression-free survival of patients with ovarian cancer in high and low lncRNA HOXA-AS3 expression groups. **P<0.01 and ***P<0.001. HOXA-AS3, HOXA cluster antisense RNA 3.

at both the mRNA and protein levels, and HOXA-AS3 interacted with HOXA3 in non-small-cell lung carcinoma cell lines (9). To evaluate the association between HOXA-AS3 and HOXA3 in ovarian cancer, RT-qPCR and western blot analyses were performed. The results revealed that knockdown of HOXA-AS3 upregulated HOXA3 expression at the mRNA and protein levels in ovarian cancer (Fig. 5A-C). In addition, immunofluorescence microscopy revealed increased HOXA3 expression in the HOXA-AS3-knockdown ovarian cancer cells (Fig. 5D). These results revealed that knockdown of HOXA-AS3 upregulated HOXA3 expression in ovarian cancer cells.

Discussion

The present study aimed to explore the functional role of HOXA-AS3 in ovarian cancer cell lines and its effect on the clinical characteristics of patients. In the present study, the knockdown of HOXA-AS3 expression was associated with decreased cell growth and migration in ovarian cancer cells. The effect of HOXA-AS3 on tumor progression may be mediated by genes involved in cell migration, invasion, and the EMT signaling pathway. The findings suggest that HOXA-AS3 may be utilized as a biomarker and therapeutic target for ovarian cancer.

Notably, lncRNAs have been receiving increasing attention for their possible role in cancer progression, including tumorigenesis, metastasis, and drug resistance (3,13,14). In particular, lncRNA HOXA-AS3, located on chromosome 7p15.2, was revealed to be correlated with the progression of several types of cancer, including glioma and lung cancer (7,9). HOXA-AS3 was highly expressed in glioma tissues and cell lines, and upregulated HOXA-AS3 expression was correlated with a poor prognosis in patients with glioma (7).

In addition, HOXA-AS3 was revealed to act as an oncogene in glioma by increasing cell proliferation, promoting cell migration, and inhibiting apoptosis (15). HOXA-AS3 was also significantly overexpressed in lung adenocarcinoma tissues and A549 cells. Knockdown of HOXA-AS3 was demonstrated to inhibit cancer cell proliferation, migration, and invasion (8). A previous study on lung cancer suggested that HOXA-AS3 was associated with cisplatin resistance *in vitro* and *in vivo*. In particular, HOXA-AS3 induced cisplatin resistance by interacting with HOXA3 in non-small cell lung carcinoma cells (9). Another interesting study on the underlying mechanism of HOXA-AS3 indicated that HOXA-AS3 acts as an epigenetic

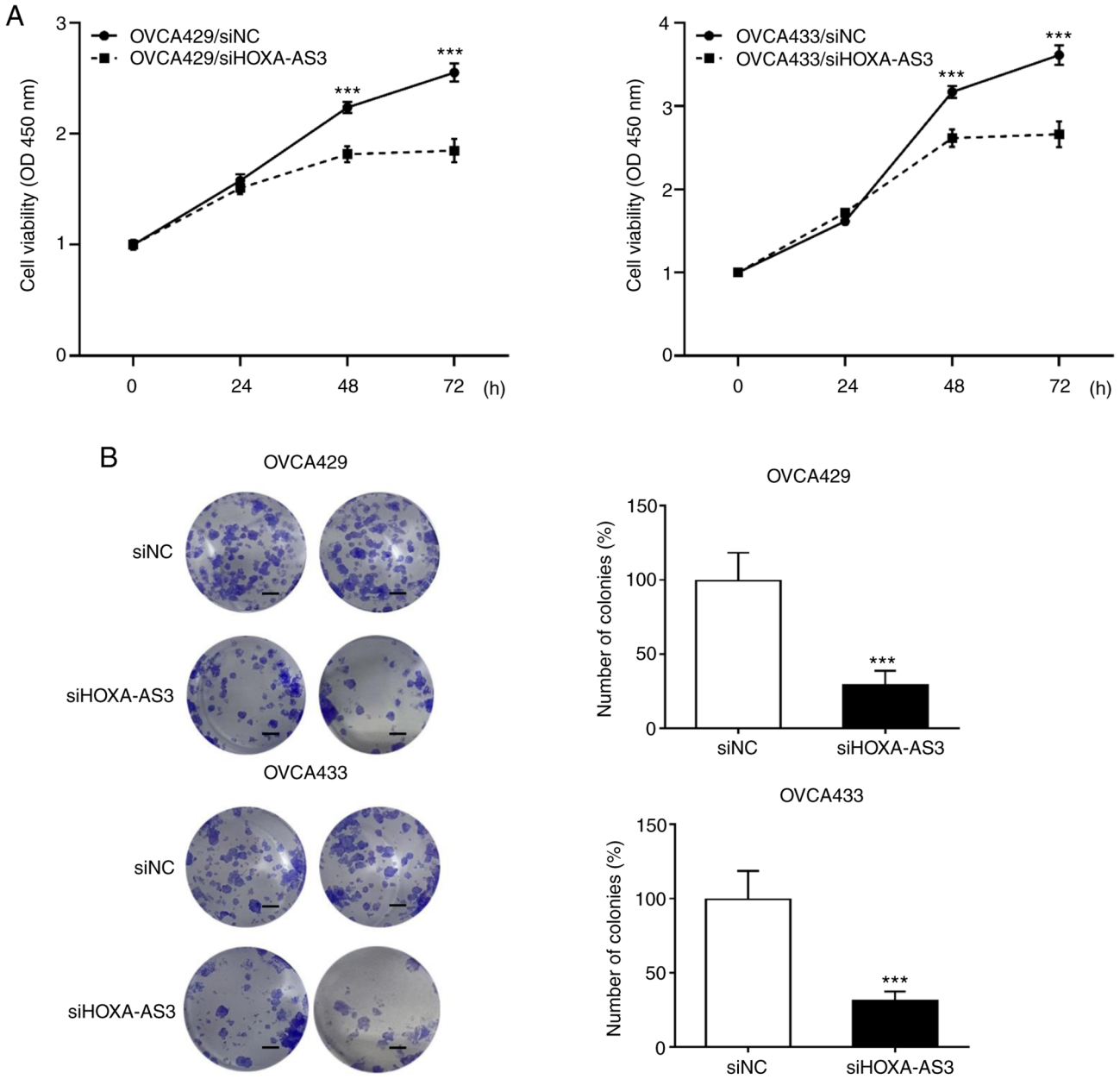

Figure 2. Knockdown of HOXA-AS3 inhibits proliferation in ovarian cancer cell lines. (A) Cell proliferation assays were performed in OVCA429 and OVCA433 cells in response to HOXA-AS3 siRNA or negative control siRNA. (B) Colony formation assays revealed that HOXA-AS3 knockdown inhibited ovarian cancer cell proliferation. Scale bar, 500 μm. ***P<0.001. HOXA-AS3, HOXA cluster antisense RNA 3; siRNA or si, small interfering RNA; NC, negative control.

switch that determines the lineage specification of mesenchymal stem cells interacting with EZH2 and is involved in H3K27me3 deposition on RUNX2, which is a key osteogenic transcription factor gene (16).

lncRNAs potentially regulate target genes through various mechanisms, including transcriptional and post-transcriptional processing, chromatin remodeling, protein functioning and localization, and intercellular signaling (17-19).

In the present study, HOXA3, which encodes for highly conserved transcription factors that are important for physiological functions, including early embryonic development, and thymus and parathyroid differentiation, was investigated (20,21). HOXA3 has various functions in the immune and nervous systems, such as promoting the differentiation of hematopoietic precursor cells into myeloid cells, regulation of macrophage activation, and prevention of aberrant neuronal identity and behavior (22-24). Particularly in tumors, HOXA3 has been reported to promote colon cancer formation by regulating the EGFR/Ras/Raf/MEK/ERK signaling pathway (25). In addition, DNA hypermethylation of HOXA3 has been identified as a potent biomarker for lung cancer (26). However, the role of HOXA3 in ovarian cancer has yet to be elucidated. In the present study, the association between HOXA-AS3 and HOXA3 was determined in ovarian cancer cell lines for the first time, to the best of our knowledge, and it was demonstrated that HOXA-AS3 is associated with cancer progression.

A previous study reported that HOXA3 induces migration and angiogenesis of endothelial and epithelial

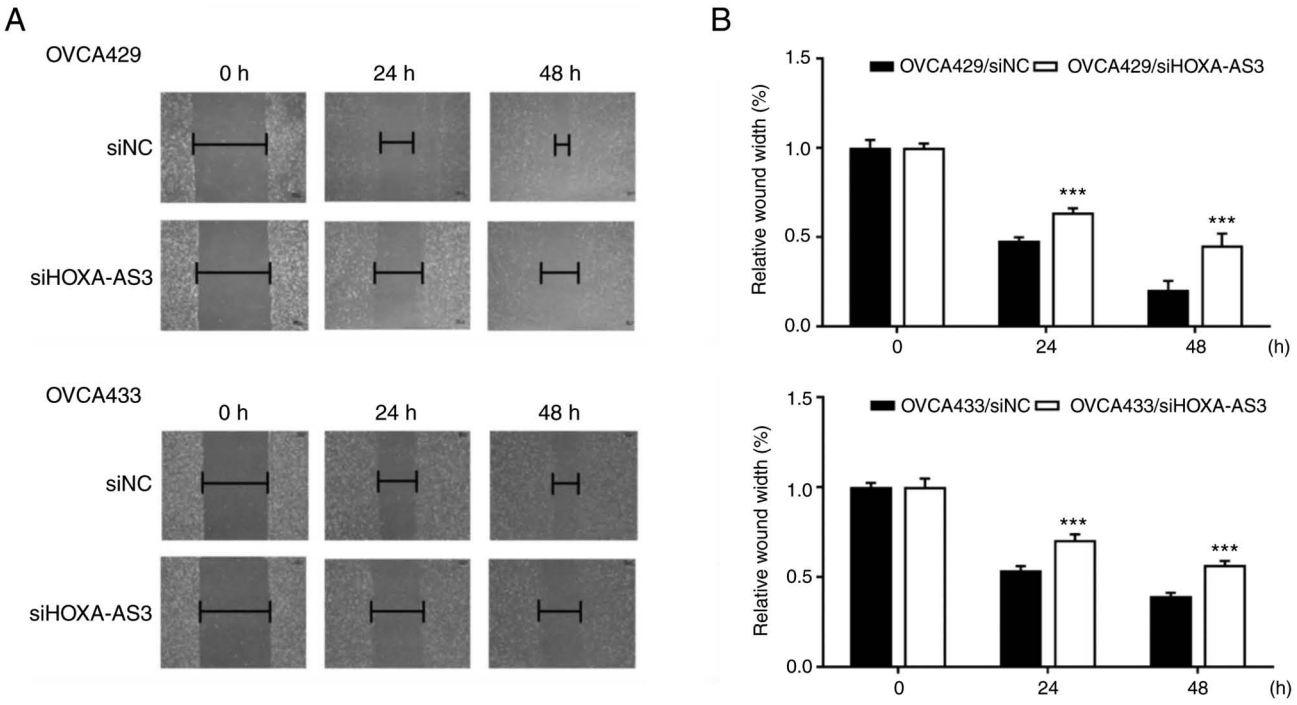

Figure 3. Knockdown of HOXA-AS3 inhibits migration in ovarian cancer cell lines. (A) Cell migration under HOXA-AS3 knockdown was evaluated by wound healing assays. (B) Quantitative analysis of wound healing rate of three independent experiments for OVCA429 and OVCA433 cell lines, using ImageJ software. Scale bar, 500 μm. ***P<0.001. HOXA-AS3, HOXA cluster antisense RNA 3; si, small interfering RNA; NC, negative control.

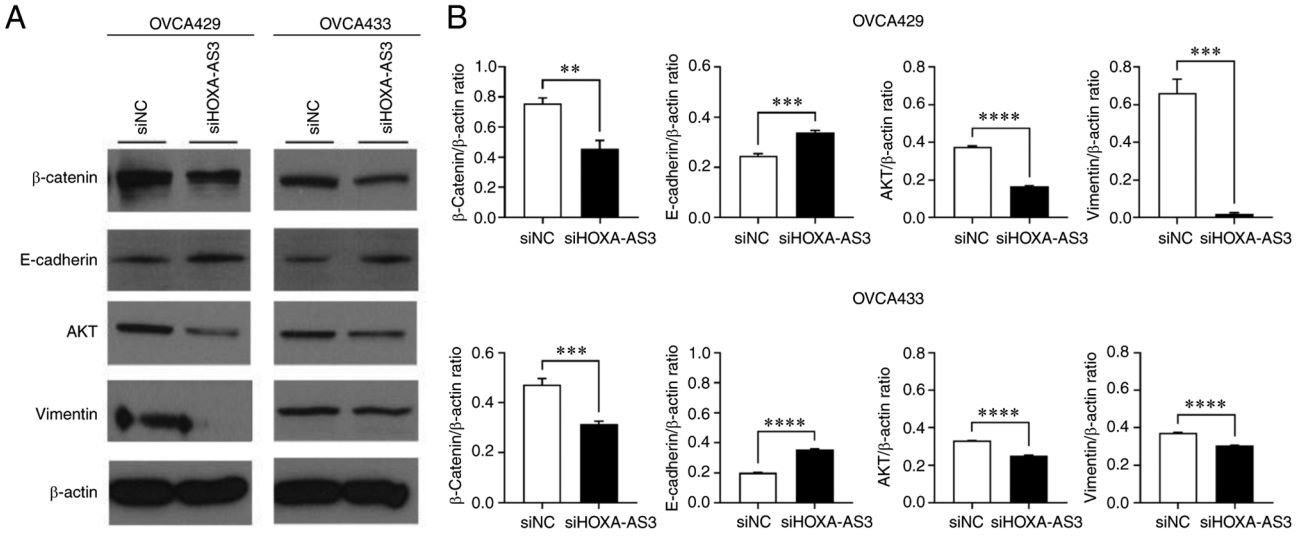

Figure 4. Knockdown of lncRNA HOXA-AS3 suppresses the epithelial-mesenchymal transition in ovarian cancer cell lines. The mRNA expression levels of E-cadherin, N-cadherin and β-catenin were analyzed using reverse transcription-quantitative polymerase chain reaction, following knockdown of lncRNA HOXA-AS3 in (A) OVCA429 or OVCA433 cells, compared with negative control siRNA. (B) Quantitative analysis of western blots of three independent experiments for OVCA429 and OVCA433 cell lines, using ImageJ software. **P<0.01, ***P<0.001 and ****P<0.0001. HOXA-AS3, HOXA cluster antisense RNA 3; siRNA or si, small interfering RNA; NC, negative control.

cells in response to injury (27). In addition, HOXA3 was reported to be an important modulator of EMT in a mouse model of idiopathic pulmonary fibrosis (7). EMT has been revealed to play an important role in tumor progression in numerous types of malignancies, including breast, lung, colon, pancreatic, and ovarian cancers (28-30). Therefore, the EMT pathway is a possible target for anticancer treatment (31,32). Furthermore, suppression of HOXA-AS3 downregulated β-catenin, AKT, vimentin, and upregulated E-cadherin expression levels, indicating that HOXA-AS3 knockdown advanced the progression of ovarian cancer cells by inducing EMT.

The present study has some limitations. Further research is required to fully elucidate the mechanism of HOXA-AS3-mediated ovarian cancer cell proliferation and migration. First, additional studies are needed to investigate other possible mechanisms and signaling pathways that may be involved in the process by which HOXA-AS3 induces cancer

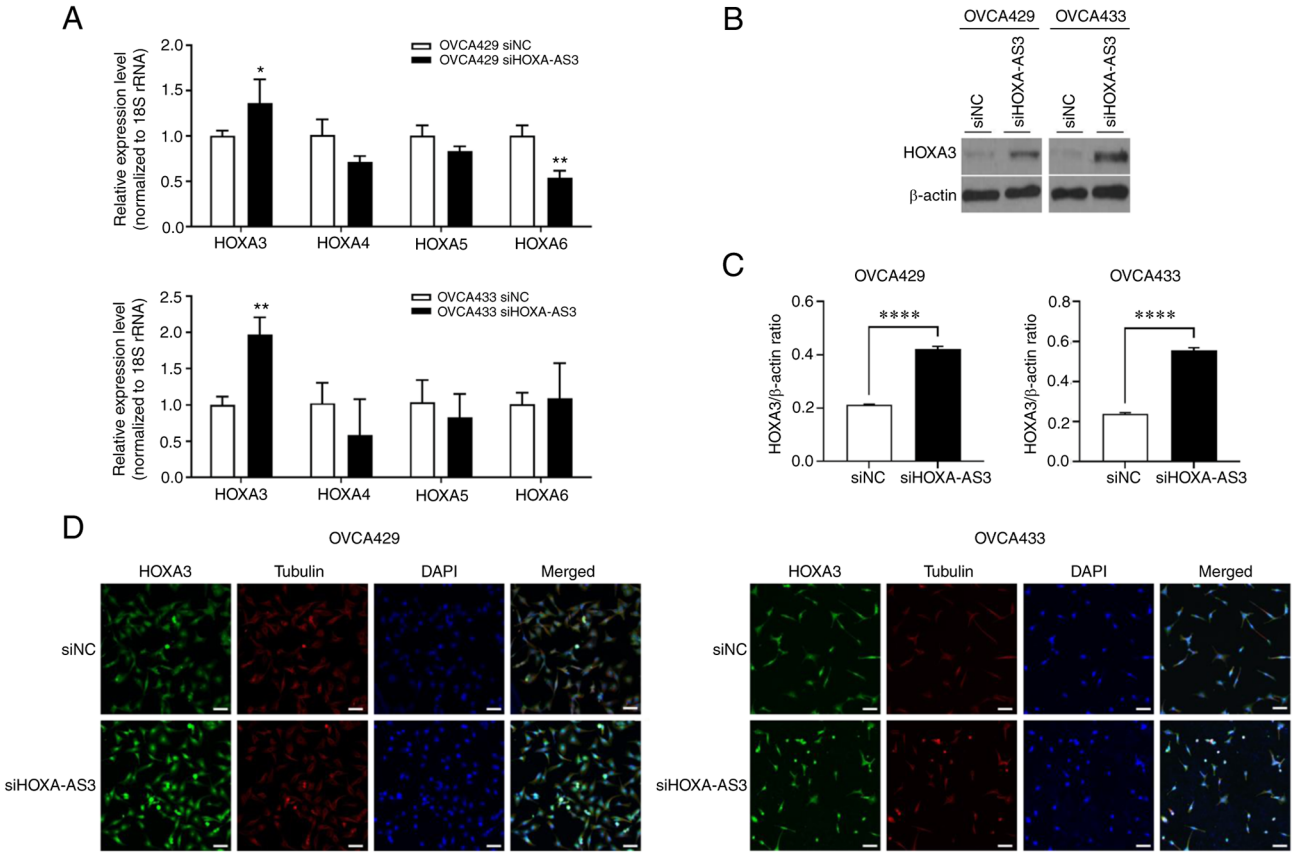

Figure 5. HOXA-AS3 regulates both HOXA3 mRNA and protein. (A) Quantitative polymerase chain reaction analyses of the mRNA expression of HOXA3 following knockdown of HOXA-AS3 expression for 48 h. (B) Detection of the protein levels of HOXA3 following knockdown of HOXA-AS3 expression for 48 h using western blotting. (C) Gray-scale quantification of HOXA3 protein level. (D) Immunofluorescence microscopy of HOXA3 (green) and DAPI (blue) proteins in OVCA429 and OVCA433 cells. Scale bar, 100 μm. *P<0.05, **P<0.01 and ****P<0.0001. HOXA-AS3, HOXA cluster antisense RNA 3; siRNA or si, small interfering RNA; NC, negative control.

cell proliferation and migration to ovarian cancer cells. In addition, correlations between HOXA-AS3/HOXA3 expression and detailed clinical variables, including oncologic outcomes in ovarian cancer patients, should be explored. Lastly, the mechanism by which HOXA-AS3 affects the EMT pathway should be studied in detail to provide a deeper understanding of the underlying molecular process of HOXA-AS3-mediated cancer progression.

Collectively, the results of the present study revealed that lncRNA HOXA-AS3 is associated with the motility and invasiveness of ovarian cancer cells. Specifically, lncRNA HOXA-AS3 promoted ovarian cancer progression by inducing cell migration and invasion via upregulation of EMT signaling pathway-related genes. Thus, lncRNA HOXA-AS3 may be a potential therapeutic target and prognostic marker for ovarian cancer.

Acknowledgements

Not applicable.

Funding

The present study was supported by a research grant from Yongin Severance Hospital, Yonsei University College of Medicine.

Availability of data and materials

The datasets used during the present study are available from the corresponding author upon reasonable request.

Authors' contributions

KJE and YTK conceived and designed the study. JIK performed the experiments. KJE, DWL, EJN, HM, SWK and JIK acquired and analyzed the data. KJE and YTK wrote the manuscript. DWL, EJN, HM and SWK revised the study critically for important intellectual content. KJE, JIK and YTK confirm the authenticity of all the raw data. All authors read and approved the final manuscript.

Ethics approval and consent to participate

The study was approved (approval ethics code 4-2021-1394) by the Institutional Review Board of Severance Hospital, Yonsei University College of Medicine. Individual patient consent was waived for the present study because it was a retrospective study which involved no risk to the subjects.

Patient consent for publication

Not applicable.

Competing interests

The authors declare that they have no competing interests.

References

1. Shin W, Won YJ, Yoo CW, Lim J and Lim MC: Incidence trends for epithelial peritoneal, ovarian, and fallopian tube cancer during 1999-2016: A retrospective study based on the Korean National Cancer Incidence Database. J Gynecol Oncol 31: e56, 2020.
2. Guttman M, Donaghey J, Carey BW, Garber M, Grenier JK, Munson G, Young G, Lucas AB, Ach R, Bruhn L, *et al*: lincRNAs act in the circuitry controlling pluripotency and differentiation. Nature 477: 295-300, 2011.
3. Kim HJ, Eoh KJ, Kim LK, Nam EJ, Yoon SO, Kim KH, Lee JK, Kim SW and Kim YT: The long noncoding RNA HOXA11 antisense induces tumor progression and stemness maintenance in cervical cancer. Oncotarget 7: 83001-83016, 2016.
4. Eoh KJ, Paek J, Kim SW, Kim HJ, Lee HY, Lee SK and Kim YT: Long non-coding RNA, steroid receptor RNA activator (SRA), induces tumor proliferation and invasion through the NOTCH pathway in cervical cancer cell lines. Oncol Rep 38: 3481-3488, 2017.
5. Arumugam T, Ramachandran V, Fournier KF, Wang H, Marquis L, Abbruzzese JL, Gallick GE, Logsdon CD, McConkey DJ and Choi W: Epithelial to mesenchymal transition contributes to drug resistance in pancreatic cancer. Cancer Res 69: 5820-5828, 2009.
6. Fischer KR, Durrans A, Lee S, Sheng J, Li F, Wong ST, Choi H, El Rayes T, Ryu S, Troeger J, *et al*: Epithelial-to-mesenchymal transition is not required for lung metastasis but contributes to chemoresistance. Nature 527: 472-476, 2015.
7. Wu F, Zhang C, Cai J, Yang F, Liang T, Yan X, Wang H, Wang W, Chen J and Jiang T: Upregulation of long noncoding RNA HOXA-AS3 promotes tumor progression and predicts poor prognosis in glioma. Oncotarget 8: 53110-53123, 2017.
8. Zhang H, Liu Y, Yan L, Zhang M, Yu X, Du W, Wang S, Li Q, Chen H, Zhang Y, *et al*: Increased levels of the long noncoding RNA, HOXA-AS3, promote proliferation of A549 cells. Cell Death Dis 9: 707, 2018.
9. Lin S, Zhang R, An X, Li Z, Fang C, Pan B, Chen W, Xu G and Han W: LncRNA HOXA-AS3 confers cisplatin resistance by interacting with HOXA3 in non-small-cell lung carcinoma cells. Oncogenesis 8: 60, 2019.
10. Yim GW, Lee DW, Kim JI and Kim YT: Long Non-coding RNA LOC285194 promotes epithelial ovarian cancer progression via the apoptosis signaling pathway. In Vivo 36: 121-131, 2022.
11. Eoh KJ, Kim HJ, Lee JW, Kim LK, Park SA, Kim HS, Kim YT and Koo PJ: E2F8 induces cell proliferation and invasion through the Epithelial-mesenchymal transition and notch signaling pathways in ovarian cancer. Int J Mol Sci 21: 5813, 2020.
12. Livak KJ and Schmittgen TD: Analysis of relative gene expression data using real-time quantitative PCR and the 2(-Delta Delta C(T)) method. Methods 25: 402-408, 2001.
13. Gupta RA, Shah N, Wang KC, Kim J, Horlings HM, Wong DJ, Tsai MC, Hung T, Argani P, Rinn JL, *et al*: Long non-coding RNA HOTAIR reprograms chromatin state to promote cancer metastasis. Nature 464: 1071-1076, 2010.
14. Kim HJ, Lee DW, Yim GW, Nam EJ, Kim S, Kim SW and Kim YT: Long non-coding RNA HOTAIR is associated with human cervical cancer progression. Int J Oncol 46: 521-530, 2015.
15. Sun H, Chen J, Qian W, Kang J, Wang J, Jiang L, Qiao L, Chen W and Zhang J: Integrated long non-coding RNA analyses identify novel regulators of epithelial-mesenchymal transition in the mouse model of pulmonary fibrosis. J Cell Mol Med 20: 1234-1246, 2016.
16. Sun Z, Yang S, Zhou Q, Wang G, Song J, Li Z, Zhang Z, Xu J, Xia K and Chang Y: Emerging role of exosome-derived long non-coding RNAs in tumor microenvironment. Mol Cancer 17: 82, 2018.
17. Marcucci F, Stassi G and De Maria R: Epithelial-mesenchymal transition: A new target in anticancer drug discovery. Nat Rev Drug Discov 15: 311-325, 2016.
18. Tang Y, Cheung BB, Atmadibrata B, Marshall GM, Dinger ME, Liu PY and Liu T: The regulatory role of long noncoding RNAs in cancer. Cancer Lett 391: 12-19, 2017.
19. Ohana P, Bibi O, Matouk I, Levy C, Birman T, Ariel I, Schneider T, Ayesh S, Giladi H, Laster M, *et al*: Use of H19 regulatory sequences for targeted gene therapy in cancer. Int J Cancer 98: 645-650, 2002.
20. Mizrahi A, Czerniak A, Levy T, Amiur S, Gallula J, Matouk I, Abu-Lail R, Sorin V, Birman T, de Groot N, *et al*: Development of targeted therapy for ovarian cancer mediated by a plasmid expressing diphtheria toxin under the control of H19 regulatory sequences. J Transl Med 7: 69, 2009.
21. Gofrit ON, Benjamin S, Halachmi S, Leibovitch I, Dotan Z, Lamm DL, Ehrlich N, Yutkin V, Ben-Am M and Hochberg A: DNA based therapy with diphtheria toxin-A BC-819: A phase 2b marker lesion trial in patients with intermediate risk nonmuscle invasive bladder cancer. J Urol 191: 1697-1702, 2014.
22. Hanna N, Ohana P, Konikoff FM, Leichtmann G, Hubert A, Appelbaum L, Kopelman Y, Czerniak A and Hochberg A: Phase 1/2a, dose-escalation, safety, pharmacokinetic and preliminary efficacy study of intratumoral administration of BC-819 in patients with unresectable pancreatic cancer. Cancer Gene Ther 19: 374-381, 2012.
23. Hasenpusch G, Pfeifer C, Aneja MK, Wagner K, Reinhardt D, Gilon M, Ohana P, Hochberg A and Rudolph C: Aerosolized BC-819 inhibits primary but not secondary lung cancer growth. PLoS One 6: e20760, 2011.
24. Lavie O, Edelman D, Levy T, Fishman A, Hubert A, Segev Y, Raveh E, Gilon M and Hochberg A: A phase 1/2a, dose-escalation, safety, pharmacokinetic, and preliminary efficacy study of intraperitoneal administration of BC-819 (H19-DTA) in subjects with recurrent ovarian/peritoneal cancer. Arch Gynecol Obstet 295: 751-761, 2017.
25. Sidi AA, Ohana P, Benjamin S, Shalev M, Ransom JH, Lamm D, Hochberg A and Leibovitch I: Phase I/II marker lesion study of intravesical BC-819 DNA plasmid in H19 over expressing superficial bladder cancer refractory to bacillus Calmette-Guerin. J Urol 180: 2379-2383, 2008.
26. Smaldone MC and Davies BJ: BC-819, a plasmid comprising the H19 gene regulatory sequences and diphtheria toxin A, for the potential targeted therapy of cancers. Curr Opin Mol Ther 12: 607-616, 2010.
27. Zhu XX, Yan YW, Chen D, Ai CZ, Lu X, Xu SS, Jiang S, Zhong GS, Chen DB and Jiang YZ: Long non-coding RNA HoxA-AS3 interacts with EZH2 to regulate lineage commitment of mesenchymal stem cells. Oncotarget 7: 63561-63570, 2016.
28. Chen YG, Satpathy AT and Chang HY: Gene regulation in the immune system by long noncoding RNAs. Nat Immunol 18: 962-972, 2017.
29. Jiang C, Li X, Zhao H and Liu H: Long non-coding RNAs: Potential new biomarkers for predicting tumor invasion and metastasis. Mol Cancer 15: 62, 2016.
30. Peng WX, Koirala P and Mo YY: LncRNA-mediated regulation of cell signaling in cancer. Oncogene 36: 5661-5667, 2017.
31. Kyba M: Modulating the malignancy of Hox proteins. Blood 129: 269-270, 2017.
32. Monterisi S, Lo Riso P, Russo K, Bertalot G, Vecchi M, Testa G, Di Fiore PP and Bianchi F: HOXB7 overexpression in lung cancer is a hallmark of acquired stem-like phenotype. Oncogene 37: 3575-3588, 2018.